Establishment of a Novel Cancer-Specific Anti-HER2 Monoclonal Antibody H2Mab-250/H2CasMab-2 for Breast Cancers

Mika K Kaneko , Hiroyuki Suzuki , Yukinari Kato *

Keywords: HER2; cancer-specific monoclonal antibody; screening; epitope; flow cytometry

Article

Establishment of a Novel Cancer-Specific Anti-HER2 Monoclonal Antibody H2Mab-250/H2CasMab-2 for Breast Cancers

Mika K. Kaneko, Hiroyuki Suzuki and Yukinari Kato *

Department of Antibody Drug Development, Tohoku University Graduate School of Medicine, 2-1 Seiryo-machi, Aoba-ku, Sendai, Miyagi 980-8575, Japan; mika.kaneko.d4@tohoku.ac.jp (M.K.K.); hiroyuki.suzuki.b4@tohoku.ac.jp (H.S.)

* Correspondence: yukinari.kato.e6@tohoku.ac.jp (Y.K.); Tel.: +81-22-717-8207 (H.S. & Y.K.)

Abstract: Overexpression of human epidermal growth factor receptor 2 (HER2) in breast and gastric cancers is an important target for monoclonal antibody (mAb) therapy. All therapeutic mAbs, including anti-HER2 mAbs, exhibit adverse effects probably due to the recognition of antigens expressed in normal cells. Therefore, tumor-selective or specific mAbs can be beneficial in reducing the adverse effects. In this study, we established a novel cancer-specific anti-HER2 antibody, named H2Mab-250/H2CasMab-2 (IgG$_1$, kappa). H2Mab-250 reacted with HER2-positive breast cancer BT-474 and SK-BR-3 cells. Importantly, H2Mab-250 did not react with non-transformed normal epithelial cells (HaCaT and MCF 10A) and immortalized normal epithelial cells in flow cytometry. In contrast, most anti-HER2 mAbs, such as H2Mab-119 and trastuzumab reacted with both cancer and normal epithelial cells. Immunohistochemical analysis demonstrated that H2Mab-250 possesses much higher reactivity to the HER2-positive breast cancer tissues compared to H2Mab-119, and did not react with normal tissues, including heart, breast, stomach, lung, colon, kidney, and esophagus. The epitope mapping demonstrated that the Trp614 of HER2 domain IV mainly contributes to the recognition by H2Mab-250. H2Mab-250 could contribute to the development of chimeric antigen receptor-T or antibody-drug conjugates without adverse effects for breast cancer therapy.

Keywords: HER2; cancer-specific monoclonal antibody; screening; epitope; flow cytometry

1. Introduction

Human epidermal growth factor receptor 2 (HER2) is included in the receptor tyrosine kinase family of human epidermal growth factor receptors. To activate the downstream signaling, HER2 must either form heterodimers with other HER members and their specific ligands or self-assemble into ligand-independent homodimers when overexpressed [1]. The HER2 overexpression is observed in approximately 20% of breast cancers [2] and 20% of gastric cancers [3], which are associated with higher rates of recurrence, poor prognosis, and shorter overall survival. A monoclonal antibody (mAb) against HER2, trastuzumab, exhibited an anti-proliferating effect *in vitro* and a potent antitumor effect *in vivo* [4,5]. The addition of trastuzumab to chemotherapy improves objective response rates, progression-free survival, and overall survival in HER2-positive breast cancer patients with metastasis [6]. Trastuzumab has become the standard treatment for HER2-positive breast cancers [7] and HER2-positive gastric cancers [8]. Trastuzumab has been the most effective therapy for HER2-positive breast cancer for more than 20 years [9].

The major adverse effect associated with anti-HER2 therapeutic mAbs is cardiotoxicity, thereby necessitating routine cardiac monitoring in clinics [10]. Furthermore, mice lacking *ErbB2* (ortholog of HER2) displayed embryonic lethal due to the dysfunctions associated with a lack of cardiac trabeculae [11]. Ventricular-restricted *ErbB2*-deficient mice showed the features of dilated cardiomyopathy [12]. These results indicate that HER2 is vital for normal heart development and

homeostasis. Therefore, more selective anti-HER2 mAbs against tumors, which can reduce heart failures are required.

We previously established several anti-HER2 mAbs, such as H_2Mab-19 (IgG_{2b}, kappa) [13], H_2Mab-41 (IgG_{2b}, kappa) [14], H_2Mab-77 (IgG_1, kappa) [15], H_2Mab-119 (IgG_1, kappa) [16], H_2Mab-139 (IgG_1, kappa) [17], and H_2Mab-181 (IgG_1, kappa) [18] by the immunization of HER2 ectodomain (HER2ec). We further engineered the mAbs into the mouse IgG_{2a} type (H_2Mab-77-mG_{2a}, H_2Mab-119-mG_{2a}, and H_2Mab-139-mG_{2a}, respectively), and produced the core fucose-deficient types (H_2Mab-77-mG_{2a}-f, H_2Mab-119-mG_{2a}-f, and H_2Mab-139-mG_{2a}-f, respectively) to potentiate the antibody-dependent cellular cytotoxicity (ADCC) and antitumor effect *in vivo* [19–21]. In this study, we developed and characterized a novel HER2 mAb, named H_2Mab-250/H_2CasMab-2.

2. Materials and Methods

2.1. Cell culture

Chinese hamster ovary (CHO)-K1, BT-474, SK-BR-3, MDA-MB-468, MCF 10A, hTERT TIGKs, HBEC3-KT, hTERT-HME1, RPTEC/TERT1, and P3X63Ag8U.1 (P3U1) were obtained from the American Type Culture Collection (ATCC, Manassas, VA). Human keratinocyte HaCaT was purchased from Cell Lines Service GmbH (Eppelheim, Germany). hTCEpi, hTEC/SVTERT24-B, and HCEC-1CT were purchased from EVERCYTE (Vienna, Austria).

The cDNA of HER2 (wild type; WT) and deletion mutants (dN218, dN342, and dN511) were cloned into the pCAG-nPA16 vector. A HER2 point mutant (W614A) and HER2 WT were cloned into the pCAG-nPA-cRAPMAP vector. CHO-K1 cells were transfected with the above-mentioned vectors using a Neon transfection system (Thermo Fisher Scientific Inc., Waltham, MA). A few days after transfection, PA tag-positive cells were sorted by the cell sorter (SH800; Sony Corp., Tokyo, Japan) using NZ-1, which was originally developed as an anti-human PDPN mAb [22]. Finally, CHO/HER2 and CHO/HER2 (dN218, dN342, dN511, and W614A) cell lines were established.

CHO-K1, CHO/HER2 (WT, deletion, and point mutants), and P3U1 were cultured in Roswell Park Memorial Institute (RPMI)-1640 medium (Nacalai Tesque, Inc., Kyoto, Japan), and BT-474, SK-BR-3, MDA-MB-468, HEK293T, and HaCaT were cultured in Dulbecco's Modified Eagle Medium (DMEM) medium (Nacalai Tesque, Inc.), supplemented with 10% heat-inactivated fetal bovine serum (FBS; Thermo Fisher Scientific Inc.), 100 units/mL of penicillin, 100 μg/mL streptomycin, and 0.25 μg/mL amphotericin B (Nacalai Tesque, Inc.). Mammary epithelial cell line, MCF 10A was cultured in Mammary Epithelial Cell Basal Medium BulletKit™ (Lonza, Basel, Switzerland) supplemented with 100 ng/mL cholera toxin (Sigma-Aldrich Corp., St. Louis, MO).

Immortalized normal epithelial cell lines were maintained, as follows; hTERT TIGKs, Dermal Cell Basal Medium and Keratinocyte Growth Kit (ATCC); HBEC3-KT, Airway Epithelial Cell Basal Medium and Bronchial Epithelial Cell Growth Kit (ATCC); hTERT-HME1, Mammary Epithelial Cell Basal Medium BulletKit™ without GA-1000 (Lonza); hTCEpi, KGMTM-2 BulletKit™ (Lonza); hTEC/SVTERT24-B, OptiPROTM SFM and GlutaMAX™-I (Thermo Fisher Scientific Inc.); RPTEC/TERT1, DMEM/F-12 and hTERT Immortalized RPTEC Growth Kit with supplement A and B (ATCC); HCEC-1CT, DMEM / M199 (4:1, Thermo Fisher Scientific Inc.), 2 % Cosmic Calf Serum (Cytiva, Marlborough, MA), 20 ng/mL hEGF (Sigma-Aldrich Corp.), 10 μg/mL insulin (Sigma-Aldrich Corp.), 2 μg/mL apo-transferrin (Sigma-Aldrich Corp.), 5 nM sodium-selenite (Sigma-Aldrich Corp.), 1 μg/mL hydrocortisone (Sigma-Aldrich Corp.).

All cell lines were cultured at 37°C in a humidified atmosphere with 5% CO_2 and 95% air.

2.2. Development of hybridomas

The animal was housed under specific pathogen-free conditions. All animal experiments were approved by the Animal Care and Use Committee of Tohoku University (Permit number: 2022MdA-001).

Anti-HER2 mAbs, such as H_2Mab-19 (IgG_{2b}, kappa) [13], H_2Mab-41 (IgG_{2b}, kappa) [14], H_2Mab-77 (IgG_1, kappa) [15], H_2Mab-119 (IgG_1, kappa) [16], H_2Mab-139 (IgG_1, kappa) [17], and H_2Mab-181

(IgG$_1$, kappa) [18] were established previously. In this study, H$_2$Mab-193 (IgG$_1$, kappa), H$_2$Mab-215 (IgG$_1$, kappa), and H$_2$Mab-250 (IgG$_1$, kappa) were established by the same strategy. Briefly, BALB/c mice were immunized with recombinant HER2ec produced by LN229 cells together with Imject Alum (Thermo Fisher Scientific, Inc.). After several additional immunizations, spleen cells were fused with P3U1 cells. The culture supernatants of hybridomas were screened using enzyme-linked immunosorbent assay (ELISA) with recombinant HER2ec and flow cytometry with cell lines.

2.3. Production of recombinant mAbs

To generate recombinant H$_2$Mab-250 and H$_2$Mab-119, their V$_H$ cDNAs and the C$_H$ cDNA of mouse IgG$_1$ were cloned into the pCAG-Neo vector (FUJIFILM Wako Pure Chemical Corporation, Osaka, Japan). The V$_L$ cDNAs and C$_L$ cDNA of the mouse kappa light chain were also cloned into the pCAG-Ble vector (FUJIFILM Wako Pure Chemical Corporation). The vectors were transfected into ExpiCHO-S cells using the ExpiCHO Expression System (Thermo Fisher Scientific, Inc.), and Ab-Capcher (ProteNova, Kagawa, Japan) was used to purify the recombinant H$_2$Mab-250 and H$_2$Mab-119.

To generate mouse IgG$_{2a}$-type H$_2$Mab-250 (H$_2$Mab-250-mG$_{2a}$), we cloned the V$_H$ cDNA of H$_2$Mab-250 and the C$_H$ of mouse IgG$_{2a}$ into the pCAG-Neo vector. The mouse kappa light chain vector of H$_2$Mab-250 was described above. To produce the defucosylated form (H$_2$Mab-250-mG$_{2a}$-f), the vectors were transfected into BINDS-09 (fucosyltransferase 8-knockout ExpiCHO-S) cells using the ExpiCHO Expression System. H$_2$Mab-250-mG$_{2a}$-f was purified using Ab-Capcher.

2.4. Flow cytometry

Cells were collected using 0.25% trypsin and 1 mM ethylenediamine tetraacetic acid (EDTA; Nacalai Tesque, Inc.). The cells (1 × 10^5 cells/sample) were treated with mouse anti-HER2 mAbs (10 μg/mL), trastuzumab (10 μg/mL), NZ-1 (10 μg/mL), or blocking buffer [control; 0.1% bovine serum albumin (BSA) in phosphate-buffered saline (PBS)] for 30 min at 4°C. Next, the cells were treated with Alexa Fluor 488-conjugated anti-mouse IgG (1:1,000; Cell Signaling Technology, Danvers, MA) for mouse anti-HER2 mAbs, Alexa Fluor 488-conjugated anti-human IgG (1:1,000; Sigma-Aldrich, Corp.) for trastuzumab, or Alexa Fluor 488-conjugated anti-rat IgG (1:1,000; Cell Signaling Technology) for NZ-1 for 30 min at 4°C. The fluorescence data was collected using EC800 or SA3800 Cell Analyzer (Sony Corp), and the data were analyzed using FlowJo (BD Biosciences, Franklin Lakes, NJ).

2.5. ADCC reporter bioassay

The ADCC reporter bioassay was performed using an ADCC Reporter Bioassay kit (Promega Corporation, Madison, WI), according to the manufacturer's instructions. Target cells (BT-474 and HaCaT, 12,500 cells per well) were cultured in a 96-well white solid plate. H$_2$Mab-250-mG$_{2a}$-f and trastuzumab (Herceptin; Chugai Pharmaceutical Co., Ltd, Tokyo, Japan) were serially diluted and added to the target cells. Jurkat cells stably expressing the human FcγRIIIa receptor and a nuclear factor of activated T-cells (NFAT) response element driving firefly luciferase, were used as effector cells. The engineered Jurkat cells (75,000 cells in 25 μl) were then added and co-cultured with antibody-treated target cells at 37°C for 6 h. Luminescence using the Bio-Glo Luciferase Assay System was measured using a GloMax luminometer (Promega Corporation).

2.6. Immunohistochemical analysis

Formalin-fixed paraffin-embedded (FFPE) tissue of HER2-positive breast cancer was obtained from Sendai Medical Center [15]. Informed consent for sample procurement and subsequent data analyses was obtained from the patient or the patient's guardian at Sendai Medical Center. Normal tissues were purchased from BioChain Institute Inc. (Eureka Drive Newark, CA) or Cybrdi Inc. (Frederick, MD). The tissue sections were autoclaved in citrate buffer (pH 6.0; Nichirei Biosciences, Inc., Tokyo, Japan) for 20 min. The blocking was performed using SuperBlock T20 (Thermo Fisher Scientific Inc.). The sections were incubated with H$_2$Mab-250 (1, 0.5, or 0.1 μg/mL) and H$_2$Mab-119

(0.5 or 0.1 µg/mL), and then treated with the EnVision+ Kit for mouse (Agilent Technologies, Inc., Santa Clara, CA). The chromogenic reaction was performed using 3,3′-diaminobenzidine tetrahydrochloride (DAB; Agilent Technologies, Inc.). Counterstaining was performed using hematoxylin (FUJIFILM Wako Pure Chemical Corporation) and Leica DMD108 (Leica Microsystems GmbH, Wetzlar, Germany) was used to obtain images and examine the sections.

2.7. ELISA

Synthesized peptides covering the HER2 extracellular domain IV and point mutant peptides were synthesized by Sigma-Aldrich Corp. The peptides (10 µg/mL) and HER2ec (1 µg/mL) were immobilized on Nunc Maxisorp 96-well immunoplates (Thermo Fisher Scientific Inc.). Plate washing was performed with PBS containing 0.05% (v/v) Tween 20 (PBST; Nacalai Tesque, Inc.). After blocking with 1% (w/v) BSA in PBST, H2Mab-250 (10 µg/mL) was added to each well. Then, the wells were further incubated with peroxidase-conjugated anti-mouse immunoglobulins (1:2000 dilution; Agilent Technologies, Inc). Enzymatic reactions were conducted using One-Step Ultra TMB. The optical density at 655 nm was measured using an iMark microplate reader.

2.8. Determination of K_D via surface plasmon resonance (SPR)

Measurement of K_D between H2Mab-250 and the HER2 peptides was performed using SPR. H2Mab-250 was immobilized on the sensor chip CM5 in accordance with the manufacturer's protocol by Cytiva. Immobilization of H2Mab-250 (10 µg/mL in acetate buffer (pH 4.0); Cytiva) was carried out using an amine coupling reaction. The surface of the flow cell 2 of the sensor chip CM5 was treated with 1-ethyl-3-(3-dimethylaminopropyl)-carbodiimide and N-hydroxysuccinimide (NHS), followed by the injection of H2Mab-250. The K_D between H2Mab-250 and the peptides was determined using Biacore X100 (Cytiva). The binding signals were measured using a single-cycle kinetics method. The data were analyzed by 1:1 binding kinetics using Biacore X100 evaluation software (Cytiva) to determine the association rate constant (k_a) and dissociation rate constant (k_d) and K_D. The affinity constant (K_A) at equilibrium was calculated as $1/K_D$.

3. Results

3.1. Establishment of H2Mab-250

We immunized mice with HER2ec produced by LN229 cells. The culture supernatants of hybridomas were screened using ELISA with HER2ec. We further screened the reactivity to HER2-positive breast cancers (BT-474 and SK-BR-3) and non-transformed normal epithelial cells including HaCaT (keratinocyte) and MCF 10A (mammary gland) using flow cytometry. One of the established hybridomas, H2Mab-250 reacted with CHO/HER2, HER2-positive BT-474, and SK-BR-3 cells, but not with triple-negative MDA-MB-468 cells. H2Mab-250 did not react with HaCaT and MCF 10A cells (Figure 1A). In contrast, H2Mab-119 showed similar reactivity to both cancer and normal epithelial cells (Figure 1A).

We next investigated the difference in the reactivity to immortalized normal epithelial cells, including hTERT TIGKs (gingiva), HBEC3-KT (lung bronchus), hTERT-HME1 (mammary gland), hTCEpi (corneal), hTEC/SVTERT24-B (thymus), RPTEC/TERT1 (kidney proximal tubule), and HCEC-1CT (colon). H2Mab-250 did not react with those normal cells, while H2Mab-119 was reactive with all immortalized normal epithelial cells (Figure 1B), indicating that H2Mab-250 possesses cancer-specific reactivity against HER2.

We further compared the reactivity of H2Mab-250 with our established anti-HER2 mAbs and trastuzumab. As shown in Supplementary Figures 1 and 2, anti-HER2 domain I mAbs (H2Mab-77 [15] and H2Mab-139 [17]), anti-HER2 domain II mAbs (H2Mab-193 and H2Mab-215), anti-HER2 domain III mAbs (H2Mab-19 [13] and H2Mab-181 [18]), and anti-HER2 domain IV mAbs (H2Mab-41 [14] and trastuzumab) reacted with HER2-positive breast cancers, non-transformed normal epithelial cells, and immortalized normal epithelial cells [16]. These results indicated that H2Mab-250 exhibits an exceptional reactivity compared to other anti-HER2 mAbs.
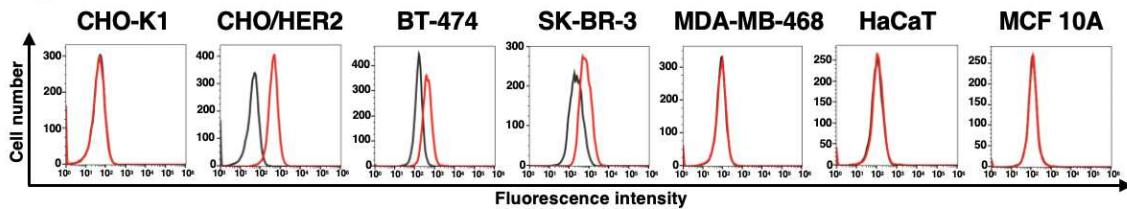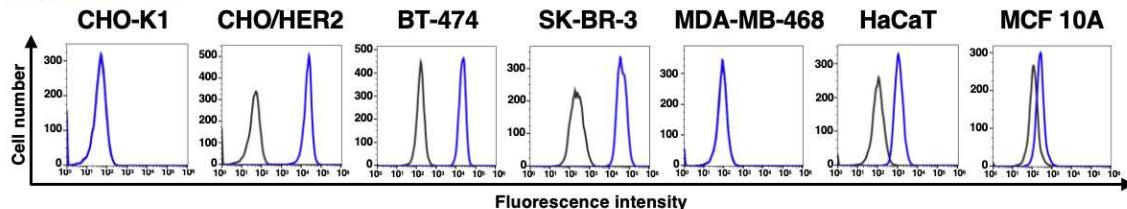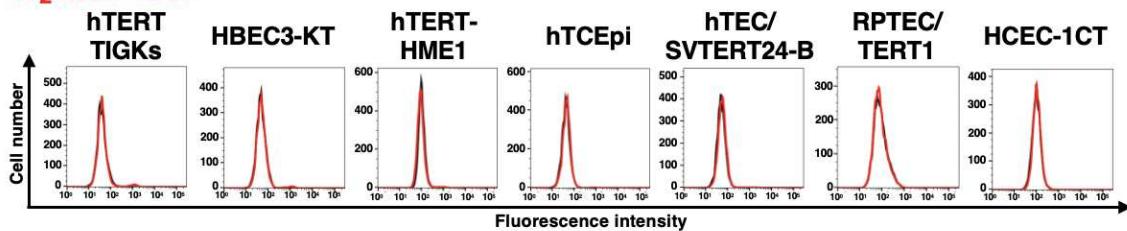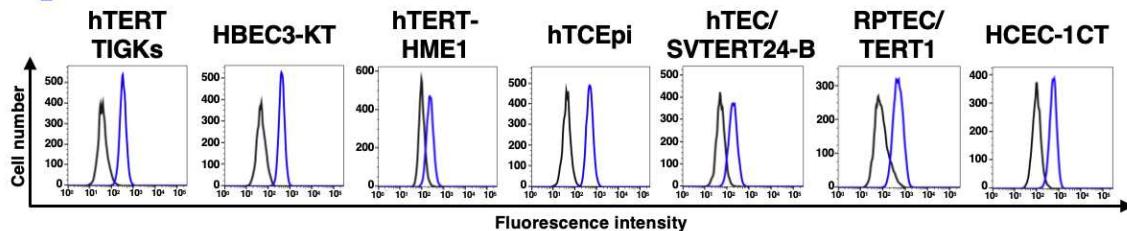
Figure 1. Flow cytometry using anti-HER2 mAbs. (A) Flow cytometry using H₂Mab-250 (10 μg/mL; Red line) and H₂Mab-119 (10 μg/mL; Blue line) against CHO-K1, CHO/HER2, HER2-positive breast cancers (BT-474 and SK-BR-3), a triple-negative breast cancer (MDA-MB-468), and non-transformed normal epithelial cells (HaCaT and MCF 10A). (B) Flow cytometry using H₂Mab-250 (10 μg/mL; Red line) and H₂Mab-119 (10 μg/mL; Blue line) against immortalized normal epithelial cells including hTERT TIGKs (gingiva), HBEC3-KT (lung bronchus), hTERT-HME1 (mammary gland), hTCEpi (corneal), hTEC/SVTERT24-B (thymus), RPTEC/TERT1 (kidney proximal tubule), and HCEC-1CT (colon). The black line represents the negative control (blocking buffer).

3.2. The ability of effector cell activation by H₂Mab-250 and trastuzumab

The ADCC reporter bioassay is a bioluminescent reporter gene assay to quantify the biological activity of the antibody via FcγRIIIa-mediated pathway activation in an ADCC mechanism of action [23]. We next produced H₂Mab-250-mG₂a-f, the core-fucose deleted IgG₂a version of H₂Mab-250 using fucosyltransferase 8-deficient ExpiCHO-S (BINDS-09) cells and examined whether H₂Mab-250-mG₂a-f could activate ADCC program in the presence of BT-474 and HaCaT cells. To compare the ADCC pathway activation by H₂Mab-250-mG₂a-f and trastuzumab, we treated BT-474 and HaCaT cells with serially diluted mAbs, and then incubated with effector Jurkat cells, which express the human

FcγRIIIa receptor and an NFAT response element driving firefly luciferase. As shown in Figure 2A, H2Mab-250-mG$_{2a}$-f could activate the effector (EC$_{50}$: 9.9 μg/mL), but it was less effective than trastuzumab (EC$_{50}$: 0.053 μg/mL). Importantly, H2Mab-250-mG$_{2a}$-f did not activate the effector in the presence of HaCaT cells. In contrast, trastuzumab activated the effector with similar EC$_{50}$ (0.036 μg/mL) to BT-474 cells (Figure 2B). These results indicated that H2Mab-250-mG$_{2a}$-f selectively activates the effector cells against breast cancer cells.
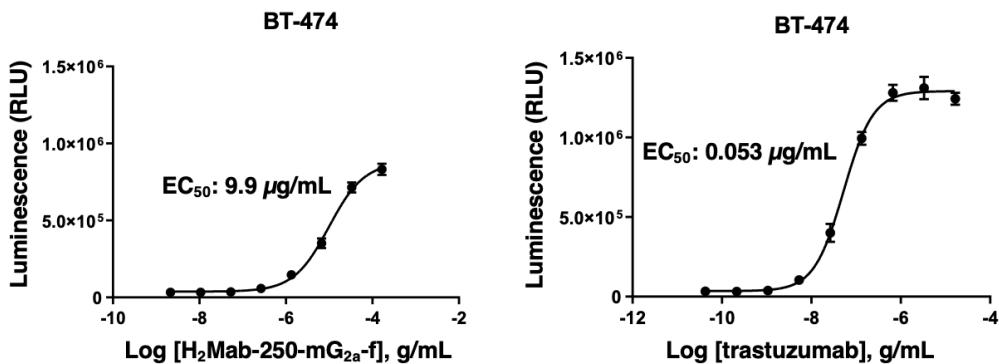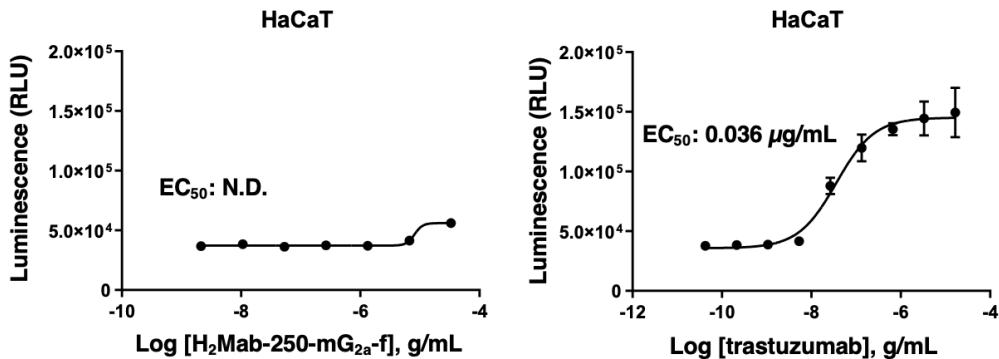
Figure 2. ADCC reporter assay by H2Mab-250-mG$_{2a}$-f and trastuzumab in the presence of BT-474 and HaCaT cells. Target cells such as BT-474 (A) or HaCaT (B) were cultured in a 96-well white solid plate. H2Mab-250-mG$_{2a}$-f and trastuzumab were serially diluted and added to the target cells. The engineered Jurkat cells were then added and co-cultured with antibody-treated target cells. Luminescence using the Bio-Glo Luciferase Assay System was measured using a GloMax luminometer. N.D., not determined. Error bars represent means ± SDs.

3.3. Immunohistochemical analysis of H2Mab-250 in breast cancer and normal epithelium

Immunohistochemical analysis was performed to examine the reactivity of H2Mab-250 with normal and tumor tissue sections. In contrast to flow cytometry, H2Mab-250 exhibited more potent reactivity to the HER2-positive breast cancer section than H2Mab-119 (Figure 3A). Since all anti-HER2 therapeutic mAbs are associated with cardiotoxicity, a major adverse effect [10], the reactivity of H2Mab-250 to a normal heart was further investigated. Even with higher concentrations of H2Mab-250 (1 μg/mL), no reactivity with the normal heart could be detected (Figure 3B). Finally, the reactivity of H2Mab-250 to other normal tissues was investigated. As shown in Figure 3C, no reactivity of H2Mab-250 with any normal tissues, including breast, stomach, lung, colon, kidney, and esophagus could be observed.
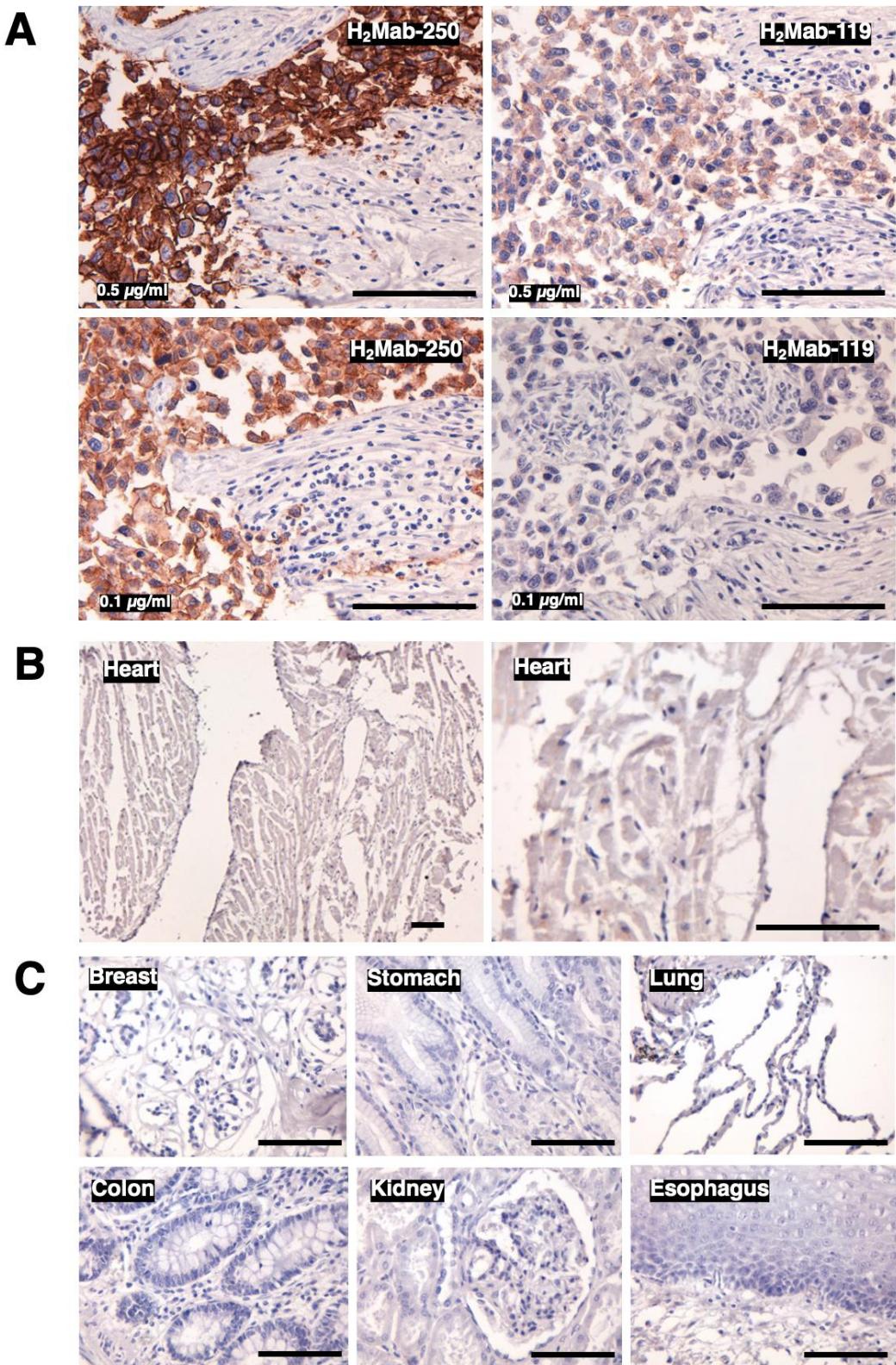
Figure 3. Immunohistochemical analysis of H₂Mab-250 in breast cancer and normal epithelium.
(A) The HER2-positive breast cancer tissue sections were treated with H₂Mab-250 or H₂Mab-119 (0.1 or 0.5 µg/mL). (B) A normal heart section was treated with H₂Mab-250 (1 µg/mL). (C) Sections of normal breast, stomach, lung, colon, kidney, and esophagus were treated with H₂Mab-250 (0.1 µg/mL). The sections were then treated with the Envision+ kit. The chromogenic reaction was performed using DAB, and the sections were counterstained with hematoxylin. Scale bar = 100 µm.

3.4. Epitope identification for H₂Mab-250

To determine the epitope for H₂Mab-250, we examined the reactivity to CHO/HER2 (WT) and the N-terminal HER2 deletion mutants (dN218, dN342, and dN511)-expressed CHO-K1 cells (Figure 4A, left). H₂Mab-250 reacted with dN218, dN342, dN511, and HER2 (WT). In contrast, H₂Mab-119 reacted with only WT, but not with dN218, dN342, and dN511. Since HER2 (WT) and the deletion mutants possess PA16 tag at the N-terminus, all expression on the cell surface could be confirmed by anti-PA16 tag mAb, NZ-1 (Figure 4A, right). These results suggest that H₂Mab-250 and H₂Mab-119 recognize the domain IV and domain I, respectively.

For further assessment of the H₂Mab-250 epitope, ELISA was performed using synthetic peptides that cover the HER2 domain IV. As shown in Figure 4B, H₂Mab-250 reacted with HER2 domain IV peptide, amino acids 603–622, 613–632, but not with 593–612, 623–642, and 633–652, indicating that H₂Mab-250 recognizes the 613–622 of HER2 domain IV. We further used alanine-substituted peptides of the 603–622 in HER2 domain IV. A potent reduction of the reactivity was observed in the W614A peptide (Figure 4C). We confirmed that the reactivity of H₂Mab-250 completely disappeared in CHO/HER2 W614A cells in flow cytometry (Figure 4D).

The K_D of H₂Mab-250 with the alanine-substituted peptides of HER2 domain IV (603–622) was measured using Biacore X100 (Table 1). The affinity constant (K_A) at equilibrium was calculated as $1/K_D$ (Figure 4E). Compared to the K_A of the 603–622 (WT) peptide, decreased K_A values were observed from the 613–617 region, suggesting that the 613–617 region is involved in the binding to H₂Mab-250. A remarkable reduction was measured in the W614A peptide, indicating that Trp614 is mainly involved in the recognition by H₂Mab-250.

Table 1. Identification of H₂Mab-250 epitope using point mutants by Biacore.

Peptide	Sequence	K_D (M)
603-622 (WT)	GVKPDLSYMPIWKFPDEEGA	5.8×10^{-9}
G603A	AVKPDLSYMPIWKFPDEEGA	5.9×10^{-9}
V604A	GAKPDLSYMPIWKFPDEEGA	6.5×10^{-9}
K605A	GVAPDLSYMPIWKFPDEEGA	6.5×10^{-9}
P606A	GVKADLSYMPIWKFPDEEGA	5.3×10^{-9}
D607A	GVKPALSYMPIWKFPDEEGA	7.1×10^{-9}
L608A	GVKPDASYMPIWKFPDEEGA	8.8×10^{-9}
S609A	GVKPDLAYMPIWKFPDEEGA	6.5×10^{-9}
Y610A	GVKPDLSAMPIWKFPDEEGA	7.9×10^{-9}
M611A	GVKPDLSYAPIWKFPDEEGA	7.5×10^{-9}
P612A	GVKPDLSYMAIWKFPDEEGA	9.5×10^{-9}
I613A	GVKPDLSYMPAWKFPDEEGA	9.4×10^{-8}
W614A	GVKPDLSYMPIAKFPDEEGA	1.1×10^{-3}
K615A	GVKPDLSYMPIWAFPDEEGA	3.4×10^{-7}
F616A	GVKPDLSYMPIWKAPDEEGA	2.0×10^{-7}
P617A	GVKPDLSYMPIWKFADEEGA	2.1×10^{-7}
D618A	GVKPDLSYMPIWKFPAEEGA	5.8×10^{-9}
E619A	GVKPDLSYMPIWKFPDAEGA	6.3×10^{-9}
E620A	GVKPDLSYMPIWKFPDEAGA	8.0×10^{-9}
G621A	GVKPDLSYMPIWKFPDEEAA	6.9×10^{-9}
A622G	GVKPDLSYMPIWKFPDEEGG	6.9×10^{-9}
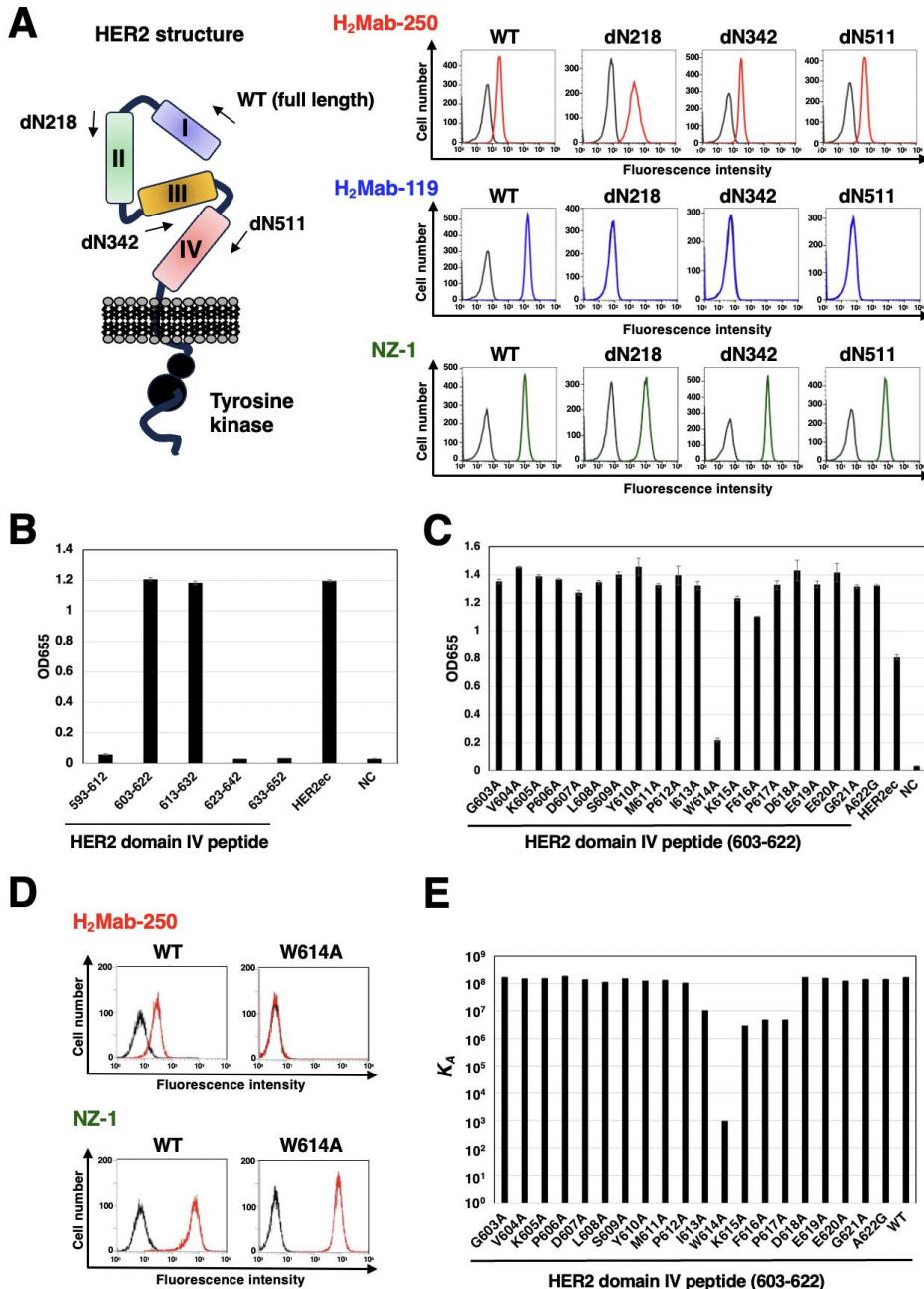
Figure 4. Epitope identification for H₂Mab-250. (A) Epitope determination of H₂Mab-250 and H₂Mab-119 using flow cytometry. The schematic representation of HER2 and the deletion mutants (left). Flow cytometry using H₂Mab-250 (10 μg/mL; Red line) and H₂Mab-119 (10 μg/mL; Blue line) against CHO/HER2 (WT and deletion mutants). The cell surface expression was confirmed by an anti-PA tag mAb, NZ-1 (10 μg/mL; Green). The cells were treated with Alexa Fluor 488-conjugated anti-mouse IgG for H₂Mab-250 and H₂Mab-119 or Alexa Fluor 488-conjugated anti-rat IgG for NZ-1. The black line represents the negative control (blocking buffer). (B and C) Determination of H₂Mab-250 epitope by ELISA. Five synthesized peptides that cover the HER2 domain IV (B), alanine-substituted peptides of HER2 domain IV (603–622) (C), HER2ec, or buffer control (NC) were immobilized on immunoplates. The plates were incubated with H₂Mab-250 (10 μg/mL), followed by incubation with peroxidase-conjugated anti-mouse immunoglobulins. Optical density was measured at 655 nm. Error bars represent means ± SDs. (D) Flow cytometry using H₂Mab-250 (10 μg/mL; Red line) against CHO/HER2 (WT and W614A). The cell surface expression was confirmed by an anti-PA tag mAb, NZ-1 (10 μg/mL; Red line). The black line represents the negative control (blocking buffer). (E) Surface plasmon resonance analysis between H₂Mab-250 and HER2 domain IV (603–622) peptides. The affinity constant (K_A) at equilibrium was calculated as $1/K_D$.

4. Discussion

In this study, we developed a cancer-specific mAb targeting HER2. H$_2$Mab-250 can recognize breast cancer cells, but not normal cells in flow cytometry (Figure 1) and immunohistochemistry (Figure 3). H$_2$Mab-250-mG$_{2a}$-f could activate ADCC against breast cancer cells, but not against normal epithelial cells (Figure 2). We also identified the H$_2$Mab-250 epitope sequence ($_{613}$-IWKFP-$_{617}$) by SPR analysis (Figure 4). The $_{613}$-IWKFP-$_{617}$ sequence is partially included with the wider binding epitope of trastuzumab (residues 579-625) [24]. Furthermore, no reaction was observed between H$_2$Mab-250 and CHO/HER2 W614A in flow cytometry (Figure 4), indicating that Trp614 plays a central role in recognition by H$_2$Mab-250. Although H$_2$Mab-250 possesses a high affinity to epitope-containing peptide (603–622) in SPR analysis, the recognition in flow cytometry using cell lines was lower than that of H$_2$Mab-119 (Figure 1). In contrast, H$_2$Mab-250 exhibited a higher reactivity than H$_2$Mab-119 in the immunohistochemical analysis using breast cancer tissues (Figure 3). This discrepancy might be induced by the possibility that the epitope sequence is partially exposed in cancer cells, but not in normal cells in clinical cancer tissues. The mechanism of recognition by H$_2$Mab-250 should be further investigated in future studies.

For the clinical treatment of metastatic breast cancer, trastuzumab is administered in patients with HER2-overexpressing tumors, which are defined by strong and complete IHC membranous staining of more than 10% of cells (IHC 3+) and/or *in situ* hybridization (ISH)-amplified. Furthermore, trastuzumab-based antibody-drug conjugates (ADCs) such as trastuzumab-deruxtecan (T-DXd) have been evaluated in various clinical trials. Based on the studies, T-DXd has been approved in not only HER2-positive breast cancers [25,26], but also HER2-mutant lung cancer [27] and HER2-low (IHC 1+ or IHC 2+ / ISH-non-amplified) advanced breast cancer [28]. A significant number of patients can benefit from T-DXd therapy since approximately half of all breast cancers are classifiable as HER2-low [29]. Meanwhile, cardiotoxicity is the most significant toxicity associated with T-DXd [30]. Further studies are essential to evaluate *in vivo* toxicities of H$_2$Mab-250.

H$_2$Mab-250-mG$_{2a}$-f could trigger the ADCC activity to BT-474 selectively (Figure 2). Although the effect of H$_2$Mab-250-mG$_{2a}$-f is lower than that of trastuzumab, we should consider that effector Jurkat cells express human FcγRIIIa receptor. In contrast, H$_2$Mab-250 exhibited a superior reactivity to HER2-positive breast cancer tissue sections in immunohistochemistry (Figure 3). Chimeric antigen receptor (CAR)-T cell therapy against HER2 has been evaluated in clinical studies [29]. It would be worthwhile to investigate the cancer specificity of H$_2$Mab-250 scFv and the efficacy of CAR-T against HER2-positive tumors in future studies. In the future, H$_2$Mab-250 could contribute to the development of CAR-T or ADCs without adverse effects for breast cancer therapy.

Supplementary Materials: The following supporting information can be downloaded at the website of this paper posted on Preprints.org.

References

1. Yarden, Y.; Sliwkowski, M.X. Untangling the ErbB signalling network. *Nat Rev Mol Cell Biol* **2001**, *2*, 127-137. https://doi.org/10.1038/35052073.
2. Slamon, D.J.; Clark, G.M.; Wong, S.G.; Levin, W.J.; Ullrich, A.; McGuire, W.L. Human breast cancer: correlation of relapse and survival with amplification of the HER-2/neu oncogene. *Science* **1987**, *235*, 177-182. https://doi.org/10.1126/science.3798106.
3. Van Cutsem, E.; Bang, Y.J.; Feng-Yi, F.; Xu, J.M.; Lee, K.W.; Jiao, S.C.; Chong, J.L.; López-Sanchez, R.I.; Price, T.; Gladkov, O.; et al. HER2 screening data from ToGA: targeting HER2 in gastric and gastroesophageal junction cancer. *Gastric Cancer* **2015**, *18*, 476-484. https://doi.org/10.1007/s10120-014-0402-y.
4. Cho, H.S.; Mason, K.; Ramyar, K.X.; Stanley, A.M.; Gabelli, S.B.; Denney, D.W., Jr.; Leahy, D.J. Structure of the extracellular region of HER2 alone and in complex with the Herceptin Fab. *Nature* **2003**, *421*, 756-760. https://doi.org/10.1038/nature01392.
5. Tsao, L.C.; Force, J.; Hartman, Z.C. Mechanisms of Therapeutic Antitumor Monoclonal Antibodies. *Cancer Res* **2021**, *81*, 4641-4651. https://doi.org/10.1158/0008-5472.Can-21-1109.
6. Essadi, I.; Benbrahim, Z.; Kaakoua, M.; Reverdy, T.; Corbaux, P.; Freyer, G. HER2-Positive Metastatic Breast Cancer: Available Treatments and Current Developments. *Cancers (Basel)* **2023**, *15*. https://doi.org/10.3390/cancers15061738.

7. Slamon, D.J.; Leyland-Jones, B.; Shak, S.; Fuchs, H.; Paton, V.; Bajamonde, A.; Fleming, T.; Eiermann, W.; Wolter, J.; Pegram, M.; et al. Use of chemotherapy plus a monoclonal antibody against HER2 for metastatic breast cancer that overexpresses HER2. *N Engl J Med* **2001**, *344*, 783-792. https://doi.org/10.1056/nejm200103153441101.

8. Bang, Y.J.; Van Cutsem, E.; Feyereislova, A.; Chung, H.C.; Shen, L.; Sawaki, A.; Lordick, F.; Ohtsu, A.; Omuro, Y.; Satoh, T.; et al. Trastuzumab in combination with chemotherapy versus chemotherapy alone for treatment of HER2-positive advanced gastric or gastro-oesophageal junction cancer (ToGA): a phase 3, open-label, randomised controlled trial. *Lancet* **2010**, *376*, 687-697. https://doi.org/10.1016/s0140-6736(10)61121-x.

9. Maadi, H.; Soheilifar, M.H.; Choi, W.S.; Moshtaghian, A.; Wang, Z. Trastuzumab Mechanism of Action; 20 Years of Research to Unravel a Dilemma. *Cancers (Basel)* **2021**, *13*. https://doi.org/10.3390/cancers13143540.

10. Copeland-Halperin, R.S.; Liu, J.E.; Yu, A.F. Cardiotoxicity of HER2-targeted therapies. *Curr Opin Cardiol* **2019**, *34*, 451-458. https://doi.org/10.1097/hco.0000000000000637.

11. Lee, K.F.; Simon, H.; Chen, H.; Bates, B.; Hung, M.C.; Hauser, C. Requirement for neuregulin receptor erbB2 in neural and cardiac development. *Nature* **1995**, *378*, 394-398. https://doi.org/10.1038/378394a0.

12. Crone, S.A.; Zhao, Y.Y.; Fan, L.; Gu, Y.; Minamisawa, S.; Liu, Y.; Peterson, K.L.; Chen, J.; Kahn, R.; Condorelli, G.; et al. ErbB2 is essential in the prevention of dilated cardiomyopathy. *Nat Med* **2002**, *8*, 459-465. https://doi.org/10.1038/nm0502-459.

13. Takei, J.; Kaneko, M.K.; Ohishi, T.; Kawada, M.; Harada, H.; Kato, Y. H2Mab-19, an anti-human epidermal growth factor receptor 2 monoclonal antibody exerts antitumor activity in mouse oral cancer xenografts. *Exp Ther Med* **2020**, *20*, 846-853. https://doi.org/10.3892/etm.2020.8765.

14. Tateyama, N.; Asano, T.; Ohishi, T.; Takei, J.; Hosono, H.; Nanamiya, R.; Tanaka, T.; Sano, M.; Saito, M.; Kawada, M.; et al. An Anti-HER2 Monoclonal Antibody H2Mab-41 Exerts Antitumor Activities in Mouse Xenograft Model Using Dog HER2-Overexpressed Cells. *Monoclon Antib Immunodiagn Immunother* **2021**, *40*, 184-190. https://doi.org/10.1089/mab.2021.0025.

15. Itai, S.; Fujii, Y.; Kaneko, M.K.; Yamada, S.; Nakamura, T.; Yanaka, M.; Saidoh, N.; Chang, Y.W.; Handa, S.; Takahashi, M.; et al. H2Mab-77 is a Sensitive and Specific Anti-HER2 Monoclonal Antibody Against Breast Cancer. *Monoclon Antib Immunodiagn Immunother* **2017**, *36*, 143-148. https://doi.org/10.1089/mab.2017.0026.

16. Yamada, S.; Itai, S.; Nakamura, T.; Chang, Y.W.; Harada, H.; Suzuki, H.; Kaneko, M.K.; Kato, Y. Establishment of H(2)Mab-119, an Anti-Human Epidermal Growth Factor Receptor 2 Monoclonal Antibody, Against Pancreatic Cancer. *Monoclon Antib Immunodiagn Immunother* **2017**, *36*, 287-290. https://doi.org/10.1089/mab.2017.0050.

17. Kaneko, M.K.; Yamada, S.; Itai, S.; Kato, Y. Development of an Anti-HER2 Monoclonal Antibody H2Mab-139 Against Colon Cancer. *Monoclon Antib Immunodiagn Immunother* **2018**, *37*, 59-62. https://doi.org/10.1089/mab.2017.0052.

18. Takei, J.; Asano, T.; Tanaka, T.; Sano, M.; Hosono, H.; Nanamiya, R.; Tateyama, N.; Saito, M.; Suzuki, H.; Harada, H.; et al. Development of a Novel Anti-HER2 Monoclonal Antibody H(2)Mab-181 for Gastric Cancer. *Monoclon Antib Immunodiagn Immunother* **2021**, *40*, 168-176. https://doi.org/10.1089/mab.2021.0021.

19. Tanaka, T.; Suzuki, H.; Ohishi, T.; Kaneko, M.K.; Kato, Y. Antitumor activities against breast cancers by an afucosylated anti-HER2 monoclonal antibody H2Mab-77-mG2a-f. *Preprint* **2023**. https://doi.org/10.20944/preprints202307.0900.v1.

20. Arimori, T.; Mihara, E.; Suzuki, H.; Ohishi, T.; Tanaka, T.; Kaneko, M.K.; Takagi, J.; Kato, Y. Locally misfolded HER2 expressed on cancer cells is a promising target for development of cancer-specific antibodies *Cell Press Community Review* **2023**, dx.doi.org/10.2139/ssrn.4565236, doi:dx.doi.org/10.2139/ssrn.4565236.

21. Suzuki, H.; Ohishi, T.; Nanamiya, R.; Kawada, M.; Kaneko, M.K.; Kato, Y. Defucosylated Monoclonal Antibody (H2Mab-139-mG2a-f) Exerted Antitumor Activities in Mouse Xenograft Models of Breast Cancers against Human Epidermal Growth Factor Receptor 2. *Curr. Issues Mol. Biol.* **2023**, *45*, 7734-7748, doi:doi.org/10.3390/cimb45100488.

22. Kato, Y.; Kaneko, M.K.; Kuno, A.; Uchiyama, N.; Amano, K.; Chiba, Y.; Hasegawa, Y.; Hirabayashi, J.; Narimatsu, H.; Mishima, K.; et al. Inhibition of tumor cell-induced platelet aggregation using a novel anti-podoplanin antibody reacting with its platelet-aggregation-stimulating domain. *Biochem Biophys Res Commun* **2006**, *349*, 1301-1307. https://doi.org/10.1016/j.bbrc.2006.08.171.

23. Garvin, D.; Stecha, P.; Gilden, J.; Wang, J.; Grailer, J.; Hartnett, J.; Fan, F.; Cong, M.; Cheng, Z.J. Determining ADCC Activity of Antibody-Based Therapeutic Molecules using Two Bioluminescent Reporter-Based Bioassays. *Curr Protoc* **2021**, *1*, e296. https://doi.org/10.1002/cpz1.296.

24. Diwanji, D.; Trenker, R.; Thaker, T.M.; Wang, F.; Agard, D.A.; Verba, K.A.; Jura, N. Structures of the HER2-HER3-NRG1β complex reveal a dynamic dimer interface. *Nature* **2021**, *600*, 339-343. https://doi.org/10.1038/s41586-021-04084-z.

25.   Modi, S.; Saura, C.; Yamashita, T.; Park, Y.H.; Kim, S.B.; Tamura, K.; Andre, F.; Iwata, H.; Ito, Y.; Tsurutani, J.; et al. Trastuzumab Deruxtecan in Previously Treated HER2-Positive Breast Cancer. *N Engl J Med* **2020**, *382*, 610-621. https://doi.org/10.1056/NEJMoa1914510.

26.   Shitara, K.; Bang, Y.J.; Iwasa, S.; Sugimoto, N.; Ryu, M.H.; Sakai, D.; Chung, H.C.; Kawakami, H.; Yabusaki, H.; Lee, J.; et al. Trastuzumab Deruxtecan in Previously Treated HER2-Positive Gastric Cancer. *N Engl J Med* **2020**, *382*, 2419-2430. https://doi.org/10.1056/NEJMoa2004413.

27.   Li, B.T.; Smit, E.F.; Goto, Y.; Nakagawa, K.; Udagawa, H.; Mazières, J.; Nagasaka, M.; Bazhenova, L.; Saltos, A.N.; Felip, E.; et al. Trastuzumab Deruxtecan in HER2-Mutant Non-Small-Cell Lung Cancer. *N Engl J Med* **2022**, *386*, 241-251. https://doi.org/10.1056/NEJMoa2112431.

28.   Modi, S.; Jacot, W.; Yamashita, T.; Sohn, J.; Vidal, M.; Tokunaga, E.; Tsurutani, J.; Ueno, N.T.; Prat, A.; Chae, Y.S.; et al. Trastuzumab Deruxtecan in Previously Treated HER2-Low Advanced Breast Cancer. *N Engl J Med* **2022**, *387*, 9-20. https://doi.org/10.1056/NEJMoa2203690.

29.   Mercogliano, M.F.; Bruni, S.; Mauro, F.L.; Schillaci, R. Emerging Targeted Therapies for HER2-Positive Breast Cancer. *Cancers (Basel)* **2023**, *15*. https://doi.org/10.3390/cancers15071987.

30.   Soares, L.R.; Vilbert, M.; Rosa, V.D.L.; Oliveira, J.L.; Deus, M.M.; Freitas-Junior, R. Incidence of interstitial lung disease and cardiotoxicity with trastuzumab deruxtecan in breast cancer patients: a systematic review and single-arm meta-analysis. *ESMO Open* **2023**, *8*, 101613. https://doi.org/10.1016/j.esmoop.2023.101613.